

Levels in  $^{97}\text{Nb}$  by Means of the  $^{96}\text{Zr}(^3\text{He}, d)$  Reaction\*L. R. Medsker<sup>†</sup>

Argonne National Laboratory, Argonne, Illinois 60439

(Received 5 July 1973)

The  $^{96}\text{Zr}(^3\text{He}, d)^{97}\text{Nb}$  reaction was studied with 22-MeV  $^3\text{He}$  particles. Experimental angular distributions were analyzed by use of distorted-wave Born-approximation calculations to determine  $l$  values and spectroscopic factors. The results are compared with previous data on reactions and  $\beta$  decay. The proton configurations of  $^{97}\text{Nb}$  are examined in comparison with neighboring niobium nuclei and recent theoretical results.

[ NUCLEAR REACTIONS  $^{96}\text{Zr}(^3\text{He}, d)$ ,  $E = 22$  MeV; measured  $\sigma(E_d, \theta)$ ; deduced  $^{97}\text{Nb}$  levels,  $l, j, G_{lj}$ . ]

## I. INTRODUCTION

The low-lying states in nuclei just above  $Z = 40$  and  $N = 50$  should be well described by configurations involving  $(\pi g_{9/2})$  and  $(\nu d_{5/2})$  since subshells are reasonably complete in this region. The situation away from closed shells became accessible to investigation only recently as experimental data have become available. The  $(^3\text{He}, d)$  reactions on zirconium isotopes ( $N = 50-56$ ) involve a sequence of neutron numbers suitable for studying the associated trends in proton-particle states.

Some information on about 20  $^{97}\text{Nb}_{56}$  levels, mainly below 2 MeV in excitation, was previously available<sup>1,2</sup> from measurements of  $\beta$  decay and from  $(d, n)$ ,  $(d, ^3\text{He})$ , and  $(^3\text{He}, d)$  reactions. Many

of the levels had been missed because of poor energy resolution or the presence of target contaminants. The present improved measurements with the  $(^3\text{He}, d)$  reaction provide the data for a more precise study of proton states away from closed shells.

## II. EXPERIMENTAL PROCEDURE

A 22-MeV  $^3\text{He}$  beam from the Argonne tandem Van de Graaff was used to obtain deuteron spectra at 17 angles between 8 and 61°. The outgoing deuterons were momentum analyzed with a split-pole magnetic spectrograph, and spectra were recorded on Kodak NTB emulsion plates. The exposed plates were scanned by a computer-controlled plate scanner.<sup>3</sup> The target, which had been

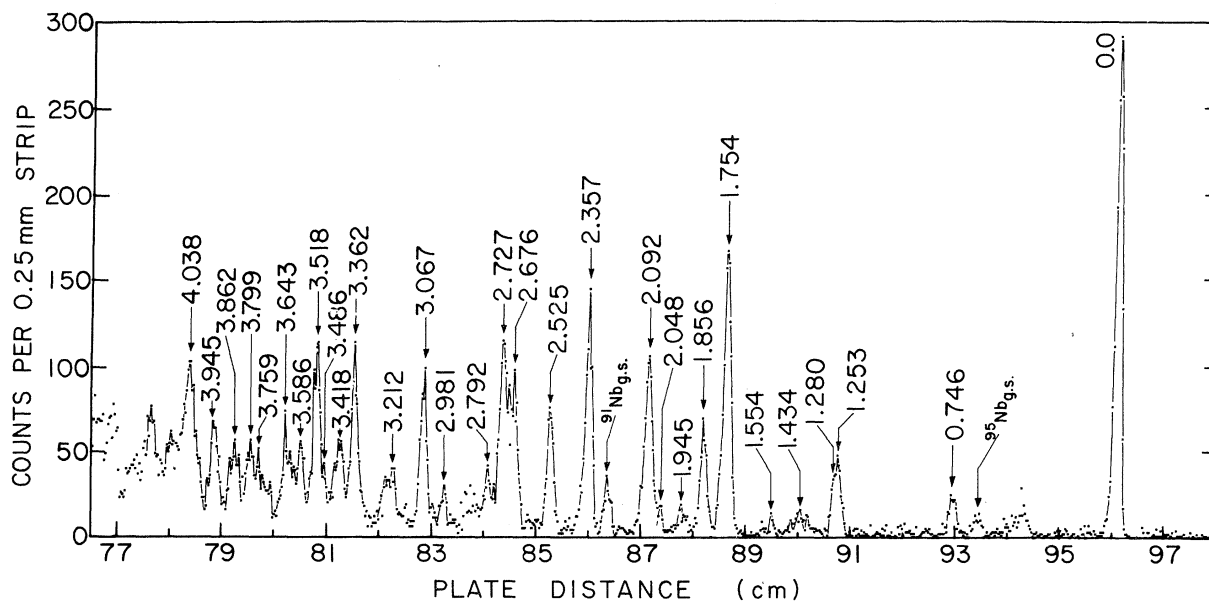


FIG. 1. Typical deuteron spectrum of the  $^{96}\text{Zr}(^3\text{He}, d)^{97}\text{Nb}$  reaction at  $\theta_{\text{lab}} = 21^\circ$ ,  $E = 22$  MeV.

TABLE I. Optical-model parameters used in distorted-wave Born-approximation calculations of  $^{96}\text{Zr}(^3\text{He}, d)^{97}\text{Nb}$ .

	$^3\text{He}$	$d$	Bound-state particle
$V$ (MeV)	172	68.8	
$r_0$ (fm)	1.14	1.033	1.2
$a$ (fm)	0.72	0.986	0.65
$W$ (MeV)	17	0	
$W_D$ (MeV)	0	11	
$r'_0$ (fm)	1.55	1.415	
$a'$ (fm)	0.8	0.716	
$r_c$ (fm)	1.4	1.3	1.4
$V_{so}$ (MeV)	0	5.34	$\lambda=25$

rolled to a thickness of approximately  $170 \mu\text{g}/\text{cm}^2$ , was enriched to 85.25% in  $^{96}\text{Zr}$ . The main contaminants were  $^{90}\text{Zr}$  (7.25%),  $^{94}\text{Zr}$  (3.85%),  $^{92}\text{Zr}$  (2.24%), and  $^{91}\text{Zr}$  (1.41%). Although the ground states of the  $^{91}\text{Nb}$  and  $^{95}\text{Nb}$  final nuclei were identified in the spectra, the strengths of their excited states were negligibly small. The over-all resolution of the system was 25 keV full width at half maximum. A typical spectrum is shown in Fig. 1.

The data were analyzed with the program

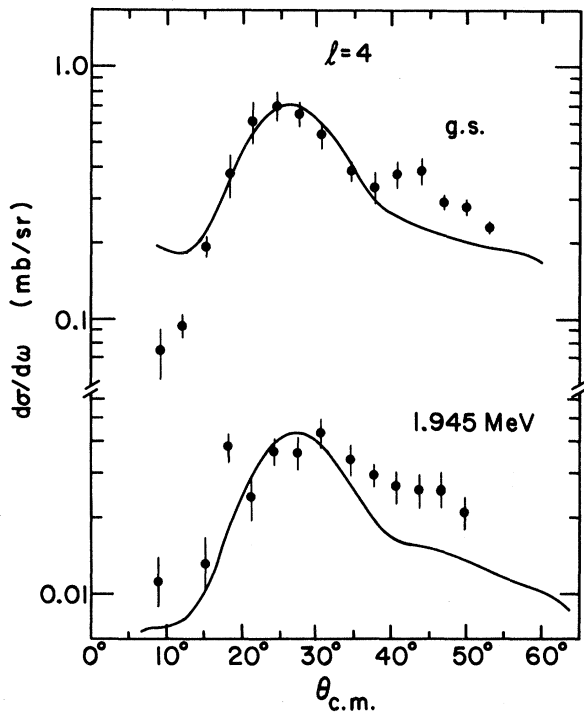


FIG. 2. Angular distributions of the deuterons leading to the ground state and the 1.945-MeV state in the  $^{96}\text{Zr}(^3\text{He}, d)^{97}\text{Nb}$  reaction. The solid lines are the distorted-wave Born-approximation calculations for  $l_p=4$  transfers.

TABLE II. Present results for the  $^{96}\text{Zr}(^3\text{He}, d)^{97}\text{Nb}$  reaction.

$E_{exc}$ (MeV)	$l_p$	$J^\pi$	$G_{IJ}$
0.0	4	$(\frac{9}{2})^+$	8.8
0.746	1	$(\frac{1}{2})^-$	0.27
1.253	1	$(\frac{3}{2})^-$	0.26
1.280	2	$(\frac{5}{2})^+$	0.15
1.434	(1, 3)		(0.074, 0.31)
1.554	1	$(\frac{1}{2}, \frac{3}{2})^-$	0.024
1.754	2	$(\frac{5}{2})^+$	0.66
1.776	(1)		(0.17)
1.856	2	$(\frac{5}{2})^+$	0.32
1.945	4	$(\frac{7}{2}, \frac{9}{2})^+$	0.37
2.048	(1)		(0.066)
2.092	2	$(\frac{3}{2}, \frac{5}{2})^+$	0.41
2.114	(2)	$(\frac{3}{2})^+$	(0.19)
2.357	(0)	$(\frac{1}{2})^+$	(0.15)
2.525	2	$(\frac{3}{2}, \frac{5}{2})^+$	0.20
2.676	2	$(\frac{3}{2}, \frac{5}{2})^+$	0.14
2.702	2	$(\frac{3}{2}, \frac{5}{2})^+$	0.17
2.727	2	$(\frac{3}{2}, \frac{5}{2})^+$	0.29
2.748	(2)		(0.12)
2.792	(0)	$(\frac{1}{2})^+$	(0.05)
2.981	(0)	$(\frac{1}{2})^+$	(0.03)
3.067	(2)		(0.12)
3.212	(2)		(0.075)
3.326	(1)		(0.047)
3.362	2	$(\frac{3}{2}, \frac{5}{2})^+$	0.25
3.418	2	$(\frac{3}{2}, \frac{5}{2})^+$	0.13
3.486	(2)		(0.065)
3.518	2	$(\frac{3}{2}, \frac{5}{2})^+$	0.24
3.537	(2)		(0.069)
3.586	2	$(\frac{3}{2}, \frac{5}{2})^+$	0.070
3.643	2	$(\frac{3}{2}, \frac{5}{2})^+$	0.083
3.759	(3)		(0.45)
3.799	(2)		(0.088)
3.862	2	$(\frac{3}{2}, \frac{5}{2})^+$	0.10
3.945	2	$(\frac{3}{2}, \frac{5}{2})^+$	0.13
4.038	2	$(\frac{3}{2}, \frac{5}{2})^+$	0.12

AUTOFIT<sup>4</sup> in order to obtain excitation energies ( $\pm 15$  keV) and relative cross sections. The measured angular distributions were compared with distorted-wave calculations for which the optical-model parameters listed in Table I were used in the program DWUCK.<sup>5</sup> The spectroscopic strengths  $G_{I_f} = [(2J_f + 1)/(2J_i + 1)] C^2 S_{I_f}$  were derived from the differential cross sections by use of the expression

$$\frac{d\sigma}{d\Omega} = \frac{4.42 G_{I_f} \sigma_{\text{DWUCK}}}{2j + 1},$$

where  $J_i$ ,  $J_f$ , and  $j$  are the total angular momenta of the target nucleus, the residual nucleus, and the transferred proton, respectively. The spectroscopic factors were normalized so that the sum for  $l_p = 4$  and  $l_p = 1$  transfers is 10, the number of holes expected in the  $Z = 50$  major shell for zirconium nuclei.

### III. RESULTS

With the resolution of the present experiment,  $l_p$  values could be assigned to 21 levels. The results for all of the well-resolved levels are shown in Table II.

The ground state is reached by a strong  $l_p = 4$

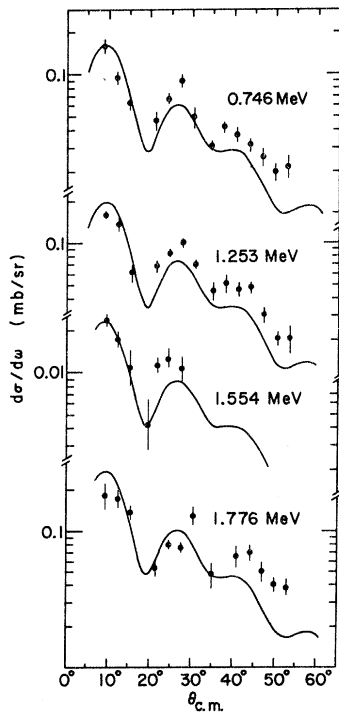


FIG. 3. Angular distributions four levels excited by  $l_p = 1$  transfer in the  $^{96}\text{Zr}({}^3\text{He}, d){}^{97}\text{Nb}$  reaction. The solid lines are the distorted-wave Born-approximation calculations.

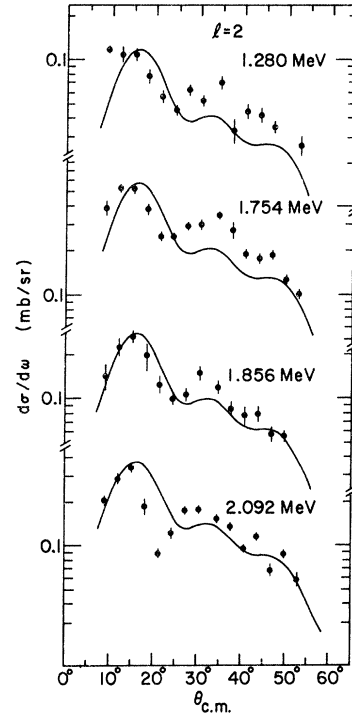


FIG. 4. Angular distributions for four levels excited in the  $^{96}\text{Zr}({}^3\text{He}, d){}^{97}\text{Nb}$  reaction. The solid lines are distorted-wave Born-approximation calculations for  $l_p = 2$  transfers.

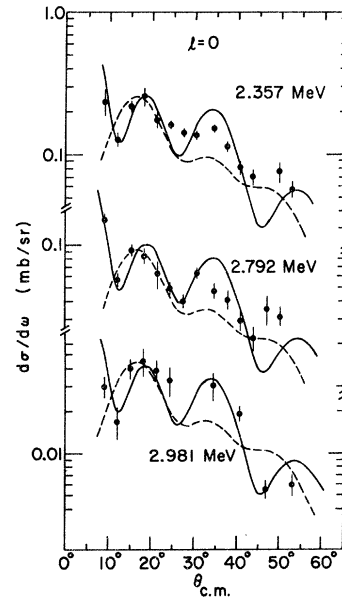


FIG. 5. Angular distributions for three levels excited by  $l_p = 0$  transfer in the  $^{96}\text{Zr}({}^3\text{He}, d){}^{97}\text{Nb}$  reaction. The results of distorted-wave Born-approximation calculations are shown with solid lines for  $l_p = 0$  and dashed lines for  $l_p = 2$ .

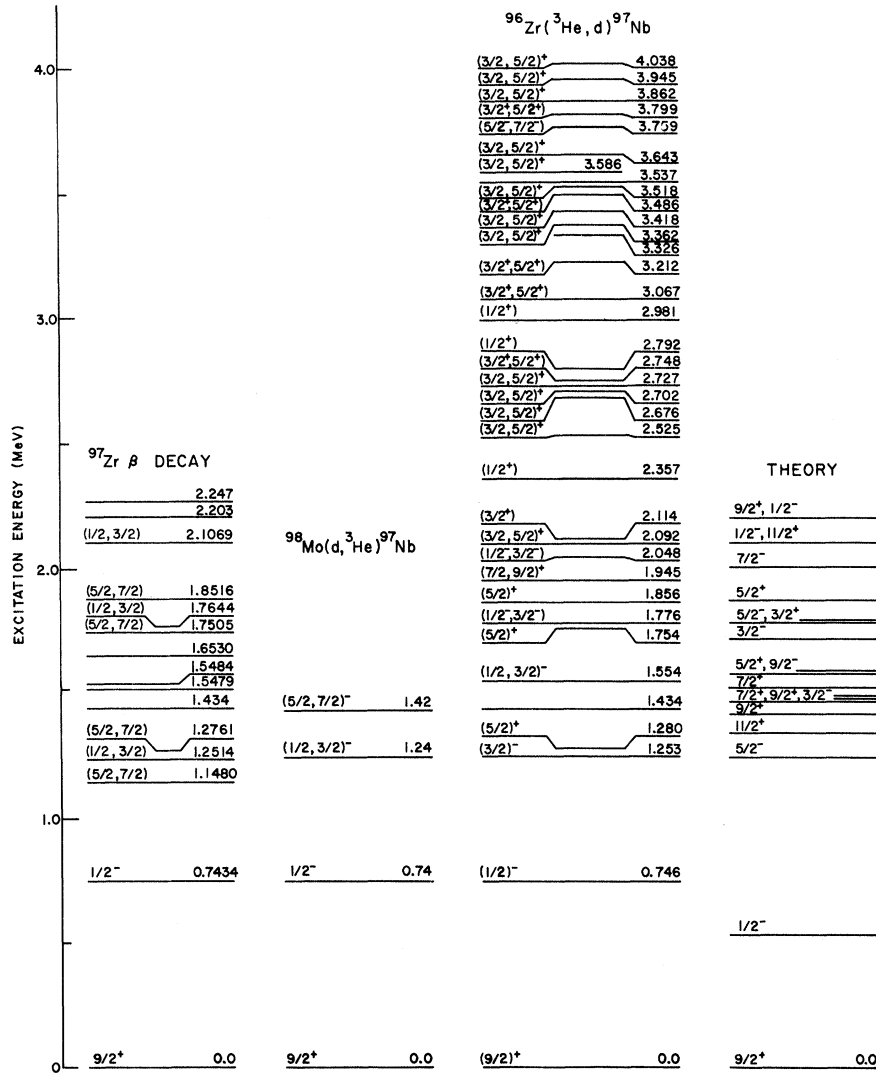


FIG. 6. Energy-level schemes of  $^{97}\text{Nb}$  as deduced from  $\beta$ -decay,  $(d, ^3\text{He})$ , and  $(^3\text{He}, d)$  measurements. The results are compared with the predictions from shell-model calculations.

TABLE III. Sums of spectroscopic strength for various  $l_p$  transfers in the  $(^3\text{He}, d)$  reactions on  $^{90, 92, 94, 96}\text{Zr}$ . The values for each isotope are normalized to a sum of 10 for the strengths of the  $l_p = 1$  and 4 transfers. The region of excitation energy  $E_x$  over which data are available is indicated in the last line. Values in parentheses are tentative results.

$l_p$	$^{90}_{40}\text{Zr}_{50}$	$^{92}_{40}\text{Zr}_{52}$	$^{94}_{40}\text{Zr}_{54}$	$^{96}_{40}\text{Zr}_{56}$
4	8.8	8.2	8.7	9.2
1	1.2	1.8	1.3	0.83
2	7.7	1.3	4.2	4.2
0	1.8			(0.23)
3			(0.14)	(0.45)
$E_x$ (MeV)	<7.1	<2.6	<3.0	<4.1

TABLE IV. Centers of gravity  $\bar{E}_i = \sum E_i G_{ij} / \sum G_{ij}$  of the level energies (MeV), observed in the  $(^3\text{He}, d)$  reactions on  $^{90, 92, 94, 96}\text{Zr}$ , for the indicated values of angular momentum. The ranges of excitation energy over which data are available are shown in the last line. Tentative results are given in parentheses.

$l_p$	$^{91}_{41}\text{Nb}_{50}$	$^{93}_{41}\text{Nb}_{52}$	$^{95}_{41}\text{Nb}_{54}$	$^{97}_{41}\text{Nb}_{56}$
4	0.07	0.05	0.0	0.089
1	0.72	0.45	0.44	0.93
2	4.7	1.7	1.8	2.7
0	5.8	(2.5)	(2.4)	(2.54)
3	(1.8)			(3.76)
$E_x$ (MeV)	<7.1	<2.6	<3.0	<4.1

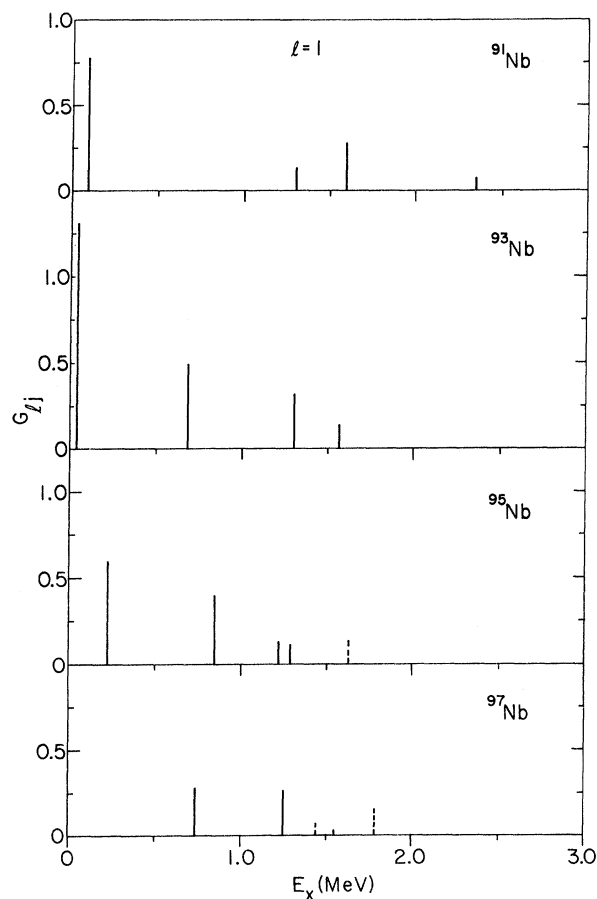


FIG. 7. Comparison of spectroscopic strengths for  $l_p = 1$  transfers to levels in niobium isotopes.

transfer (Fig. 2), consistent with the expectation that the  $g_{9/2}$  proton shell is almost empty in the  $^{96}\text{Zr}$  ground state. A small amount of additional  $l_p = 4$  strength was found at 1.945 MeV. The  $l_p = 1$  strength is distributed chiefly among levels at 0.746, 1.253, 1.554, and 1.776 MeV (Fig. 3). More than 20 states, most of them above 2 MeV excitation, were observed by  $l_p = 2$  transfers, and typical cases are shown in Fig. 4. States with energies 2.357, 2.792, and 2.981 MeV were tentatively assigned  $l_p = 0$  (Fig. 5); however,  $l_p = 2$  cannot be ruled out. The state at 3.759 is tentatively assigned  $l_p = 3$ .

In Fig. 6, the results of the present ( $^3\text{He}, d$ ) study are compared with  $\beta$ -decay and ( $d, ^3\text{He}$ ) measurements. Several levels reported in the latter two were not seen in the present study. In particular, no evidence was found for the  $\frac{7}{2}^+$  levels reported in the decay of  $^{97}\text{Zr}$ . The  $l_p = 3$  transfer to the 1.42-MeV level reported from ( $d, ^3\text{He}$ ) may possibly be identified with the 1.434-MeV level found

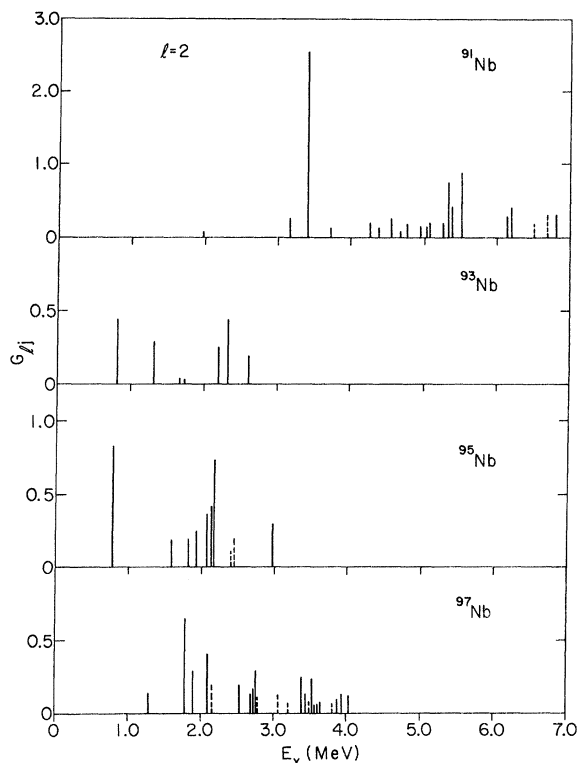


FIG. 8. Comparison of spectroscopic strengths for  $l_p = 2$  transfers to levels in niobium isotopes.

in the present ( $^3\text{He}, d$ ) measurements. That level is only weakly populated here, consistent with the  $^{96}\text{Zr}$  ground state having a nearly full  $f_{5/2}$  orbit.

No published theoretical calculations are available for comparison with the experimental data for  $^{97}\text{Nb}$ . However, in recent shell-model calculations<sup>6</sup>  $^{97}\text{Nb}$  is assumed to be a  $^{88}\text{Sr}$  core plus three protons and six neutrons. The results of preliminary calculations with  $(\pi g_{9/2})$ ,  $(\pi p_{1/2})$ ,  $(\nu d_{5/2})$ , and  $(\nu s_{1/2})$  as active orbitals are shown in Fig. 6. Similar models have been successful in predicting the approximate order and spins of low-lying states in zirconium and niobium isotopes in the region  $A = 90-96$ . The number of states with  $J^\pi = \frac{1}{2}^-$  and  $\frac{3}{2}^-$  is consistent with the number of states observed with  $l_p = 1$  transfers, but the measured strengths are much larger than predicted. The level scheme for  $^{97}\text{Nb}$  is more complex than those for isotopes closer to the  $N = 50$  closed shell; however, the calculations indicate the possibility of describing some features of the data in the context of the shell model.

The present results are summarized in Tables III and IV, where the sums of spectroscopic strengths and the energy centers of gravity are compared with the data<sup>2,7,8</sup> for other zirconium

targets. The sums of strengths are consistent with the description in which  $1g_{9/2}$ ,  $2p_{1/2}$ , and  $2p_{3/2}$  are the active orbitals in zirconium. In agreement with earlier conclusions,<sup>2</sup> the separation of the centers of gravity for  $l=4$  and  $l=1$  orbitals increases as the  $2p_{3/2}$  and  $2p_{1/2}$  orbitals become more full and the  $1g_{9/2}$  becomes more empty.

Figure 7 shows the concentration of the  $l=1$  strength in  $^{91}\text{Nb}$  and  $^{93}\text{Nb}$  and the fragmentation as neutrons are added. The comparison for  $l=2$  strength is less clear because of the absence of data for  $^{93}\text{Nb}$  and  $^{95}\text{Nb}$  in the excitation region  $E_x$

$>3$  MeV. The existing data, shown in Fig. 8, indicate increasing fragmentation as neutrons are added. Much of the  $l=2$  strength in  $^{91}\text{Nb}$  is associated with the level at 3.410 MeV. For the other isotopes, no comparable intensity of strength is observed, and states are observed about 2 MeV lower in excitation.

#### ACKNOWLEDGMENTS

The helpful advice of J. P. Schiffer during the acquisition and analysis of the data is greatly appreciated. I also thank D. Gloeckner for communicating preliminary calculations.

---

\*Work performed under the auspices of the U. S. Atomic Energy Commission.

†Present address: Physics Department, University of Pennsylvania, Philadelphia, Pennsylvania 19104.

<sup>1</sup>L. R. Medsker, Nucl. Data B10, 1 (1973).

<sup>2</sup>M. R. Cates, J. B. Ball, and E. Newman, Phys. Rev. 187, 1682 (1969).

<sup>3</sup>J. R. Erskine and R. H. Vonderohe, Nucl. Instrum. Methods 81, 221 (1970).

<sup>4</sup>J. R. Comfort, Argonne National Laboratory Physics

Division Informal Report No. PHY-1970B (unpublished).

<sup>5</sup>We are grateful to Dr. P. D. Kunz for making this program available to us.

<sup>6</sup>D. Gloeckner, private communication. See also, D. Gloeckner, Phys. Lett. 42B, 381 (1972).

<sup>7</sup>K. T. Knopfle, M. Rogge, C. Mayer-Boricke, J. Pedersen, and D. Burch, Nucl. Phys. A159, 642 (1970).

<sup>8</sup>L. R. Medsker and J. L. Yntema, Phys. Rev. C 7, 440 (1973).